KSOE
Original Research Article

Journal of Ocean Engineering and Technology 34(5), 316-324 October, 2020
https://doi.org/10.26748/KSOE.2020.054

pISSN 1225-0767
eISSN 2287-6715

Reliability Analysis for Structure Design of Automatic Ocean Salt Collector Using Sampling Method of Monte Carlo Simulation

Chang Yong Song[1]

[1]*Professor, Department of Naval Architecture and Ocean Engineering, Mokpo National University, Jeonnam, Korea*

KEY WORDS: Monte Carlo simulation, Sampling method, Reliability analysis, Meta-model, Automatic ocean salt collector

ABSTRACT: *This paper presents comparative studies of reliability analysis and meta-modeling using the sampling method of Monte Carlo simulation for the structure design of an automatic ocean salt collector (AOSC). The thickness sizing variables of structure members are considered as random variables. Probabilistic performance functions are selected from strength performances evaluated via the finite element analysis of an AOSC. The sampling methods used in the comparative studies are simple random sampling and Sobol sequences with varied numbers of sampling. Approximation methods such as the Kriging model is applied to the meta-model generation. Reliability performances such as the probability failure and distribution are compared based on the variation of the sampling method of Monte Carlo simulation. The meta-modeling accuracy is evaluated for the Kriging model generated from the Monte Carlo simulation and Sobol sequence results. It is discovered that the Sobol sequence method is applicable to not only to the reliability analysis for the structural design of marine equipment such as the AOSC, but also to Kriging meta-modeling owing to its high numerical efficiency.*

1. Introduction

Whereas the marine fishery equipment industry is expected to increase in market size worldwide as a major industry for securing food resources, the level of fishery equipment expertise in South Korea is extremely low and the ratio of localization relative to the market size is only approximately 50% (KMI, 2019). A salt collector is marine fishery equipment used to collect salt from marine salt ponds; it is an equipment that must be automated to facilitate the labor-intensive operation of salt pans. The domestic development of electrically driven automatic ocean salt collectors (AOSCs) has begun to improve the safety level during traditional marine salt collection and transfer processes as well as increase the production output per unit area of crystallization ponds. Owing to the lack of domestic and international regulations in the design of marine fishery equipment, the structural safety of new types of fishery equipment, such as AOSCs, is evaluated during the design stage by determining design load conditions that satisfy the operational requirements and applying them in the structural analysis of the equipment. However, the reliability of AOSCs' structural performances must be evaluated while considering unavoidable uncertainties in the operation of salt ponds, such as corrosion issues, to appropriately determine the safety of the structural design.

Several studies have been conducted to verify the design safety of marine fishery equipment by applying reliability analysis. Lee and Kim (2006) applied the first and second reliability analysis techniques for the reliability evaluation of pipelines and verified the reliability analysis results by comparing them to Monte Carlo simulation (MCS) results. To optimize the reliability-based design of floating production storage & offloading riser add-ons, Song et al. (2011) investigated an optimal design plan to minimize design risks by applying the constraint-feasible moving least-squares method, which is a conservative approximation model. Bai et al. (2015) performed a finite element analysis and used surface response methods for MCS-based reliability analysis on lightweight subsea pipelines. Lee and Kim (2017) calculated the probability of failure in a limit state function using first and second reliability analysis techniques to perform probabilistic defect assessments of defects inherent in mooring chains; subsequently, the probabilities of failure obtained from the limit state function and MCS were compared to verify the adequacy of the approximated probability of failure. Yin et al. (2018) developed a non-probabilistic reliability convex model for the reliability analysis and sensitivity evaluation of valve port plates of deep-sea hydraulic pumps.

Received 15 September 2020, revised 24 September 2020, accepted 25 September 2020
Corresponding author Chang Yong Song: +82-61-450-2732, cysong@mokpo.ac.kr

In this study, reliability analysis was performed by applying the general MCS and the Sobol sequence method (SSM), which is one of the quasi-MCS methods, to derive an efficient reliability evaluation method to ensure the structural design safety of AOSCs. Furthermore, the probability of reliability based on the sampling method and the accuracy of the Kriging metamodeling were compared. In the reliability analysis, the thickness of the major structural components of the AOSC were set as a random variable, while considering possible corrosions caused by the nature of the work environment; meanwhile, the strength performance was assumed as a probabilistic performance function. The strength performance of the AOSC was evaluated by calculating the design load conditions considering the actual operating conditions and applying them to the structural analysis model based on the finite element method (FEM) to calculate the maximum stress for each design load condition. To review the reliability probability, probability performance function distribution, and efficiency of numerical calculations, the SSM was used by varying the sampling frequency at a constant ratio, and the results were compared with those of the general MCS, which uses the simple random sampling method. The SSM is effective for reliability analysis owing to its excellent numerical efficiency; however, a review of reasonable sampling methods is required based on the characteristics of the analysis subject because the sampling frequency for the target confidence level is not fixed. In this study, to establish an SSM that is applicable to the analysis of fishery equipment structures, sampling methods for the SSM were investigated to achieve the results of MCS for estimating the reliability of AOSC structural design with a confidence level of 95% and an error rate of 5%. Additionally, to analyze the correlation between the design space approximation characteristics and sampling methods, the approximation accuracy was compared using Kriging metamodels suitable for approximation with random sampling data. This paper is organized as follows. The theoretical backgrounds of the MCS, SSM, and Kriging metamodeling are briefly outlined in Section 2. The FEM-based strength performance evaluation, reliability analysis result comparison, and Kriging metamodeling result comparison are presented in Section 3. Finally, the overall research findings are summarized in the Conclusions section.

2. Theoretical Background

2.1 MCS

MCS is a practical reliability analysis method to determine the uncertainties associated with random variables in a probability performance function for a suitable sampling frequency that satisfies the target confidence level in the evaluation of the probabilities of reliability or failure. However, because the MCS involves a simple random sampling method in which the sampling frequency increases with the target confidence level and accuracy, the efficiency of reliability analysis may be lower. Therefore, numerical calculation experiments, rather than physical experiments, are applied in MCS-based reliability analysis (Siddall, 1983). As shown in Fig. 1, an

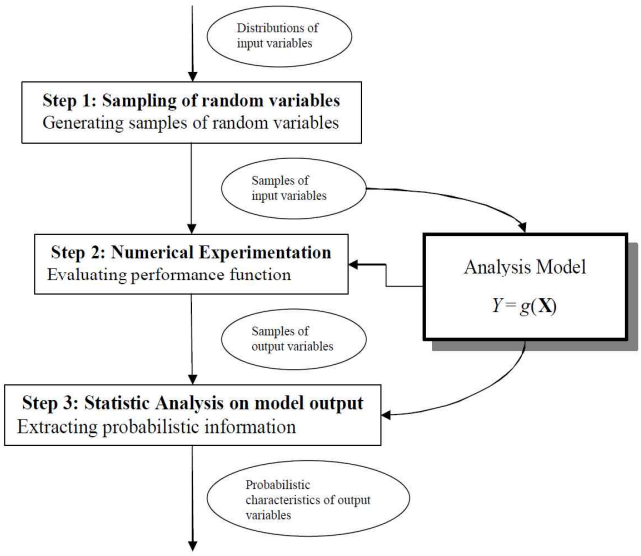

Fig. 1 Procedure of MCS

MCS is performed in three stages, i.e., sampling of random variables, numerical experimentation, and statistical analysis, for random variables $X = (X_1, X_2, \cdots, X_n)$ and a probability performance function $Y = g(X)$.

In the statistical analysis stage, the probability performance function, Y, is calculated as many times as the sampling frequency, N, to perform reliability analysis by calculating the mean $\overline{Y}$, variance σ_Y^2, and probability of failure p_f, as follows:

$$\overline{Y} = \frac{1}{N}\sum_{i=1}^{N} y_i \tag{1}$$

$$\sigma_Y^2 = \frac{1}{N-1}\sum_{i=1}^{N}\left(y_i - \overline{Y}\right)^2$$

$$p_f = P\{g \le 0\} = \int \cdots \int_{g(x) \le 0} f_{X_1, X_2, \cdots, X_n}(x_1, x_2, \cdots, x_n)\, dx_1 dx_2 \cdots dx_n$$

$$= \int_{g(x) \le 0} f_X(x)\, dx$$

where $X = (X_1, X_2, \cdots, X_n)$ and $x = (x_1, x_2, \cdots, x_n)$

The probability of failure, p_f, in Eq. (1) can be expressed using an indicator function, $I(x)$, as follows:

$$p_f = \int_{-\infty}^{+\infty} I(x) f_X(x)\, dx \tag{2}$$

$$\text{where } I(x) = \begin{cases} 1 & \text{if } g(x) \le 0 \\ 0 & \text{otherwise} \end{cases}$$

The probability of failure is arranged as follows using the mean value of the indicator function:

$$p_f = \overline{I}(x) = \frac{1}{N}\sum_{i=1}^{N} I(x_i) = \frac{N_f}{N} \tag{3}$$

Here, N_f is the sampling frequency when $g \le 0$. The probability of reliability, R, is defined as follows:

$$R = P\{g > 0\} = 1 - p_f = \frac{N - N_f}{N} \tag{4}$$

The probability of failure is obtained in terms of a cumulative distribution function (CDF), $F_Y(y)$, and a probability density function (PDF), $f_Y(y)$, as shown below:

$$F_Y(y) = P(g \le y) = \frac{1}{N}\sum_{i=1}^{N} I'(y_i) \tag{5}$$

$$\text{where } I(x) = \begin{cases} 1 & \text{if } g(x) \le y \\ 0 & \text{otherwise} \end{cases}$$

$$f_Y(y) = [F_Y(y)]'$$

As shown in Eq. (5), the PDF is a differential of the CDF. The accuracy of the MCS can be assessed as a function of error rate, e, based on the 95% confidence level as follows:

$$e\,[\%] \approx 200\sqrt{\frac{(1-p_f)}{Np_f}} \tag{6}$$

As shown in Eq. (6), once the target probability of failure and error rate are defined, the sampling frequency required for the reliability analysis can be determined. The accuracy of the probability of failure evaluated in the MCS may be improved if the sampling frequency requirement is satisfied; however, the sampling frequency should be determined based on the characteristics of the analysis subject and the efficiency of numerical calculations in engineering design.

2.2 SSM

SSM is a quasi-MCS method designed to allow a consistent sampling with a low sampling frequency of multidimensional variables in a design space (Sobol & Levitan, 1999; Saltelli et al., 2010). In the SSM, a sampling position is selected based on the previous sampling point, thereby minimizing the gap with a cluster. A Sobol sequence is generated from a combination of binary fractions with a length of w beats and the direction numbers of v_i^j, $[i = 1, 2, \cdots, w;\ j = 1, 2, \cdots, d]$. To generate directional numbers in the j dimension, the following primitive and recursive polynomials of directional numbers are defined:

$$p_j(x) = x^q + a_1 x^{q-1} + \cdots + a_{q-1}x + 1 \tag{7}$$

$$v_i^j = a_1 v_{i-1}^j \oplus a_2 v_{i-2}^j \oplus \cdots \oplus a_{q-1} v_{i-q+1}^j \oplus v_{i-q}^j \oplus \left(v_{i-q}^j / 2^q\right)$$

$$\text{where } i > q$$

In Eq. 7, $\oplus$ refers to the XOR bitwise operation. The Sobol sequence of the j dimension, $x_q^j\left(n = \sum_{i=0}^{w} b_i 2^i, b_i \in \{0, 1\}\right)$, is generated using primitive polynomials at each dimension, as follows:

$$x_n^i = b_1 v_1^j \oplus b_2 v_2^j \oplus \cdots \oplus b_w v_w^j \tag{8}$$

The sampling frequency, N_T, required in the SSM is defined as follows:

$$N_T = N_S(m+1) \tag{9}$$

$$\text{where } N_S = 2^k,\ k = 1, 2, 3, \cdots$$

m in Eq. (9) refers to the number of random variables. The sampling frequency in the SSM is not fixed and should be determined based on the complexity of the analysis subject and the number of random variables.

2.3 Kriging Metamodel

Because metamodels are generated from the sampled data in the experimental planning or design space, the accuracy of the generated metamodels can be quantitatively reviewed to verify the approximation of the design space based on the sampling method (Lee & Song, 2013). Creating a highly accurate metamodel is one of the most important tasks in the exploratory research of the design space as it can significantly reduce the numerical inefficiencies by utilizing it for multipurpose or reliability-based design optimizations that involve a high number of calculation iterations.

A Kriging model is expressed as the sum of the global model of the actual design space function to be approximated and the local model that corresponds to the difference between the actual function and the global model (Cho et al., 2009).

$$\tilde{g}(x)_K = Z(x)^T A_K + E(x) \tag{10}$$

Here, $A_K = \{a_1, a_2, \cdots, a_p\}^T$ is an unknown coefficient vector, and $Z(x) = \{z_1(x), z_2(x), \cdots, z_p(x)\}^T$ is a global model vector defined with a design variable, $x \in E^{n_d}$. The global model can be defined as $p = 1$ in a constant case, $p = n_d + 1$ in a linear case, and $p = (n_d+1)(n_d+2)/2$ in a second-order polynomial case. $E(x)$ represents an independent normal distribution, and the response vector obtained from n experimental positions is defined as follows:

$$g = [g(x^1), g(x^2), \cdots, g(x^n)]^T \tag{11}$$

$E(x)$ is a spatial correlation of the design data and is generally defined as a Gaussian correlation function, expressed as follows:

$$E(\theta, x^i, x^j) = \exp\left[-\sum_{k=1}^{n_d} \theta_k (x^i - x^j)^2\right] \tag{12}$$

Here, $\theta, x \in E^{n_d}$ and the correlation matrix is a positive definite matrix

with diagonal elements of 1. The correlation coefficient, θ_k, is a parameter that expresses the correlation of the response values in the x_k-direction and determines the curvature of the Kriging model in the x_k-direction. The correlation decreases with increasing θ_k, as shown in Eq. (12), and the approximation of the Kriging metamodel in the direction of the input variables shows nonlinear characteristics. The correlation becomes more evident with decreasing θ_k, as shown in Eq. (12), and the approximation of the Kriging metamodel in the direction of the input variables shows linear characteristics. The correlation coefficient, θ, with the highest probability can be calculated through the maximum likelihood estimation, which maximizes the likelihood function.

3. Review of Reliability Analysis

3.1 Evaluation of AOSC Strength Performance

The system configuration of the entire AOSC and the thickness of the major structural components for FEM modeling are shown in Fig. 2. As shown in Fig. 2(a), the AOSC has a salt collector and a towing unit system for automatic salt collection; a drive and power system for delivering electric drive power; a rail frame for transferring collected salt; and a collector frame, rail frame, and a main frame for the system installation and load support. As shown in the FEM analysis model in Fig. 2(b), the main frame structure was created as a shell element, the weight of each system was realized as a lumped mass, and the rigid link element was used to connect each structural component and apply the lumped mass and design load. The thicknesses of the main frame, rail frame, collector frame, and bracket were designed to be 6.0, 1.0–3.0, 1.0, and 4.0 mm, respectively. The FEM model contained 112,896 elements and 114,431 nodes with the following material properties applied: a density of 8,000 kg/m^3, elastic modulus of 193 GPa, the Poisson's ratio of 0.29, and a yield strength of 216 MPa, as in austenitic stainless steel (SUS316).

During the initial design phase, the design load conditions for the AOSC strength performance evaluation were determined by combining the system weight and operating load to reflect the worst-case scenario and by selecting the maximum loading conditions as well as the operating and braking conditions under the maximum load, as listed in Table 1. The inertial load in the direction of gravity, the acceleration of operating conditions in the transfer direction, and the acceleration of the braking conditions in the opposite direction of transfer were applied. The design load conditions listed in Table 1 were applied in the FEM analysis, and all degrees of freedom were

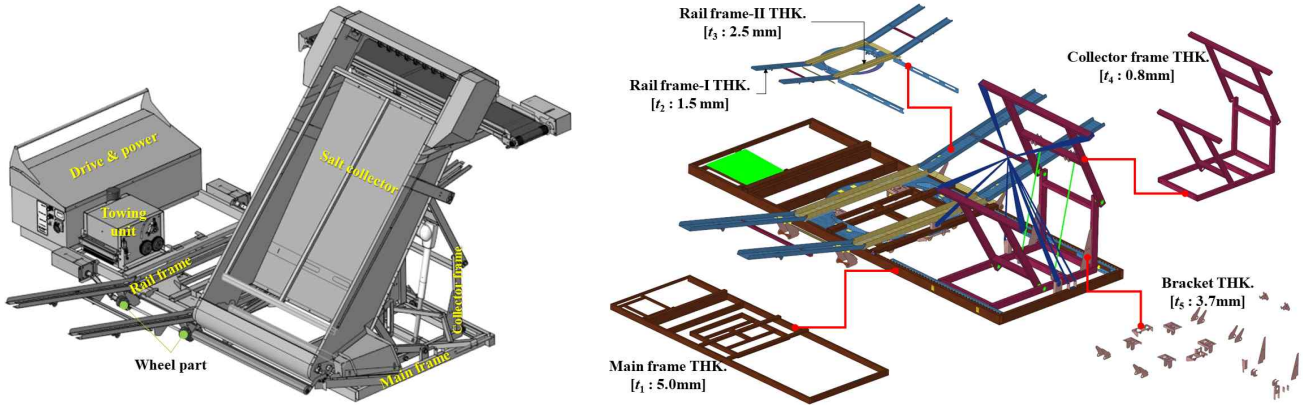

(a) System configuration (b) FEM model

Fig. 2 System configuration and structure analysis model

Table 1 Design load cases

Design loads	Load cases		
	Loading [LC1]	Operating [LC2]	Braking [LC3]
Salt collector weight (0.2 t)	√	√	√
Drive & power part weight (0.23 t)	√	√	√
Towing part weight (0.07 t)	√	√	√
Wheel part weight (0.03 t)	√	√	√
Inertial load (1.0 G[1])	√	√	√
Max. salt collecting capacity (0.7 t)	√	√	√
Max. towing capacity (490 N)	-	√	-
Acceleration at operating (1.25 G)	-	√	-
Acceleration at braking (-1.25 G)	-	-	√

[1]G (gravitaional acceleration): 9.8 m/s^2

Table 2 Structure analysis results

Structure part	Max. von-Mises stress (MPa)			Safety check
	LC1	LC2	LC3	
Overall structure	166.2	149.2	173.8	OK
Main frame	**166.2**	142.0	164.2	OK
Rail frame	151.7	**149.2**	155.5	OK
Collector frame	51.0	55.4	54.1	OK
Bracket	159.9	139.7	**173.8**	OK

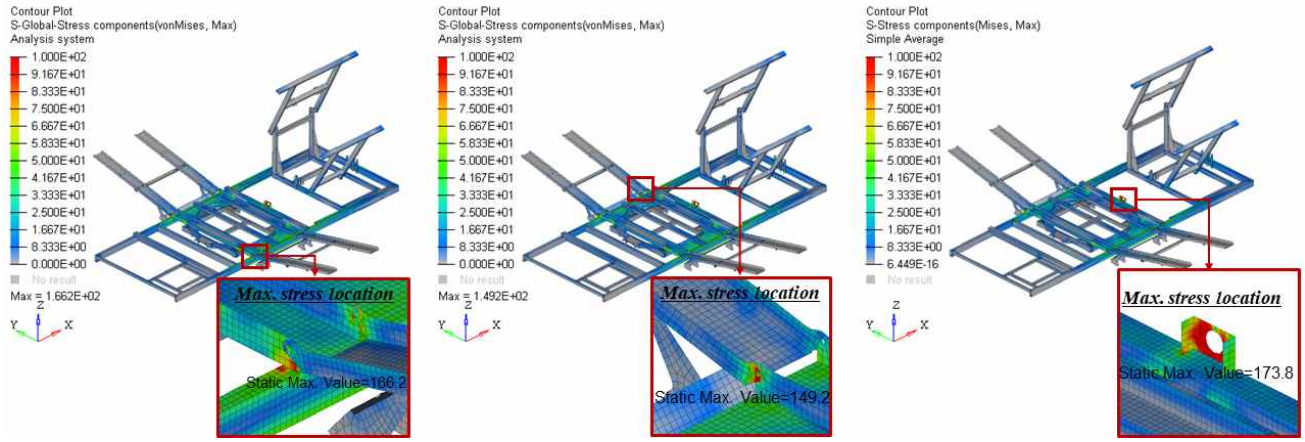

(a) LC1 (b) LC2 (c) LC3

Fig. 3 Stress contour results (unit: MPa)

restricted for the boundary conditions, except for the degree of freedom associated with the rotation of each wheel mounted at the bottom of the rail. As shown in Table 2, the general-purpose finite element analysis program, Abaqus/Implicit (Simulia, 2018), was used in the FEM analysis to calculate the maximum von Mises stress for each design load condition and evaluate the structural safety based on the yield stress of the material. The structure was considered to be safe if the maximum stress under each design load condition was less than 85% of the yield stress, or 183 MPa (DNV-GL, 2015). As outlined in Table 2, the structural safety was adequate in all of the design load conditions, with the highest stress of 173.8 MPa occurring at the bracket part in LC3. The structural components with the highest stress were the main frame part in LC1, rail frame part in LC2, and bracket part in LC3, whereas the collector frame part in all of the load conditions indicated the lowest stress level.

The stress distribution result for each design load condition is shown in Fig. 3. The maximum stress in LC1 occurred at the main frame part connected to the rail frame, the maximum stress in LC2 was at the rail frame connection, and the maximum stress in LC3 was at the center of the bracket. The maximum stress occurred at the center of the bracket part in LC3 because the weight of the salt collector part and the weight of the collected salt concentrated at the center, resulting in a high level of load under the braking conditions. Whereas the strength performance of the AOSC structural design satisfied the structural safety standard, a safety margin of less than 5% before reaching the performance limit was indicated in LC3; therefore, a quantitative reliability review is necessary to address uncertainties in the design factors.

3.2 Reliability Analysis of AOSC Structural Design

Unlike marine structures that have design regulations regarding corrosion allowance, an AOSC is a fishery equipment with insufficient design regulations. Because AOSCs are used in marine salt ponds and their material thickness is the design factor, corrosion can be considered as a key uncertainty. Therefore, in the reliability evaluation of AOSCs, the thickness of the major structural components was set as

Table 3 Random variables

Random variable	RSD	Distribution type	Design variable	Mean
X_1	10 %	Normal	Main frame (t_1)	5.0 mm
X_2	10 %	Normal	Rail frame-I (t_2)	1.5 mm
X_3	10 %	Normal	Main frame-II (t_3)	2.5 mm
X_4	10 %	Normal	Collector frame (t_4)	0.8 mm
X_5	10 %	Normal	Bracket (t_5)	3.7 mm

Table 4 Comparison of reliability analysis results

Sampling method		# of sampling	Probability of reliability (≤183 MPa)		
			LC1	LC2	LC3
MCS		158,400	96.1 %	99.7 %	91.9 %
SSM	Case 1	6,144	96.1 %	99.7 %	91.9 %
	Case 2	3,072	96.1 %	99.7 %	92.0 %
	Case 3	1,536	96.1 %	99.7 %	91.9 %
	Case 4	768	96.3 %	99.9 %	92.3 %
	Case 5	384	96.5 %	99.9 %	92.4 %
	Case 6	192	96.9 %	100 %	92.5 %
	Case 7	96	97.9 %	100 %	92.9 %

a random variable to account for corrosions that may be caused by the nature of the work environment, whereas the strength performance was considered as a probability performance function. To address the uncertainty around the thickness of the structural components as a random variable, the mean was set to the initial design thickness, and the relative standard deviation (RSD) was set as 10% based on the experimental study results pertaining to the corrosion properties of austenitic stainless steel (Han and Park, 2012); furthermore, they were defined to follow a normal distribution because the variability in the strength performance with corrosion was reviewed for a normal operation of the AOSC in this study. The settings of the random variables used in the reliability analysis are listed in Table 3.

In this study, the limit of the strength performance as a probability performance function was set to be 183 MPa, which is the standard for structural safety, whereas the reliability of the structural design was evaluated based on a probability of failure, p_f, of 0.01. Reliability analysis was performed based on the MCS and SSM. The sampling frequency in the MCS was set to 158,400 based on Eq. (6) with a 95% confidence level and an error rate of 5%. The frequency of sampling in the SSM was varied sequentially by changing the constant k in Eq. (9)

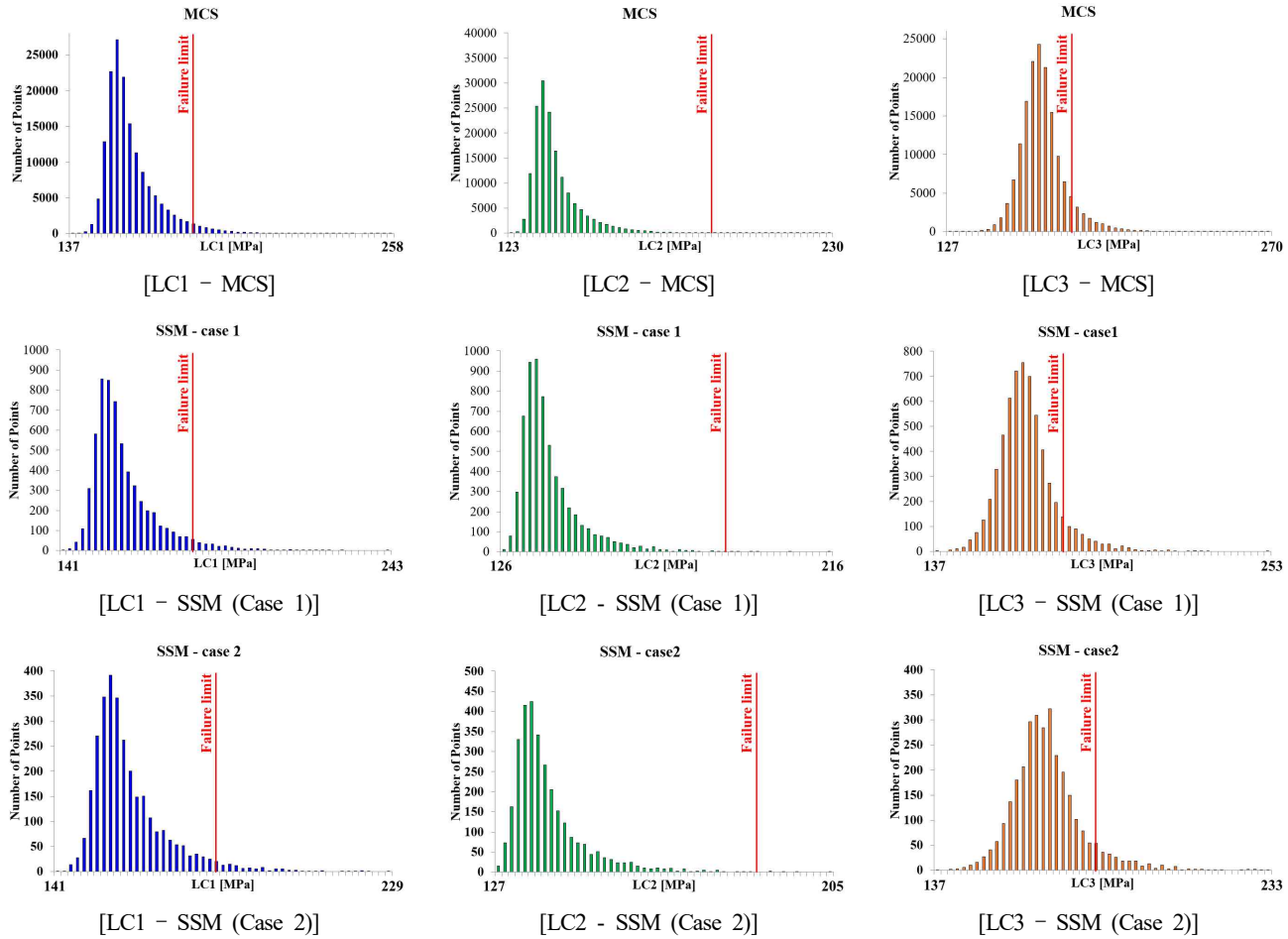

Fig. 4 Comparison of PDF results (continuation)

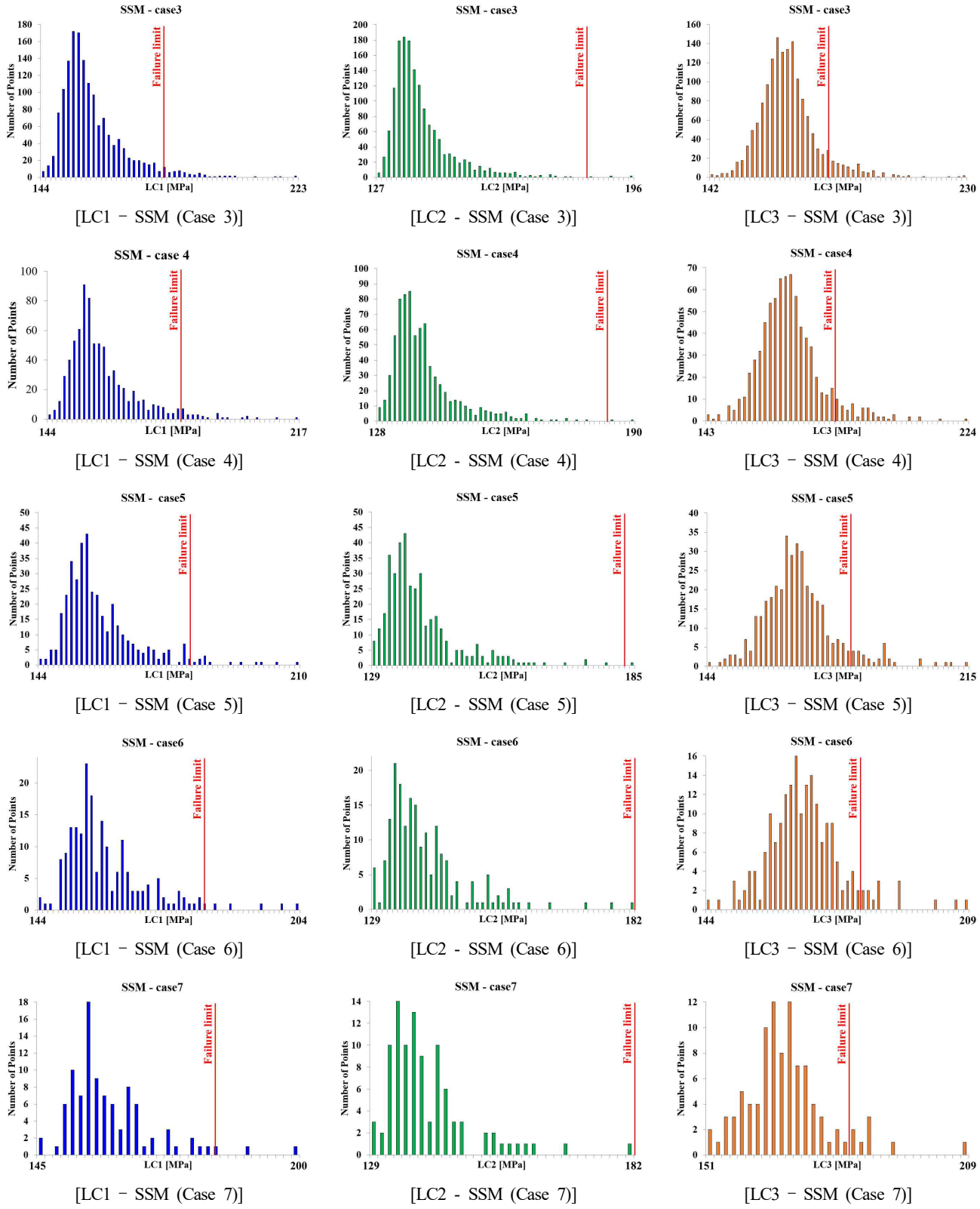

Fig. 4 Comparison of PDF results

from 10 to 4, for the following seven cases: 6,144 (Case 1), 3,072 (Case 2), 1,536 (Case 3), 768 (Case 4), 384 (Case 5), 192 (Case 6), and 96 (Case 7). The results of reliability analysis based on the MCS and SSM with varying sampling frequency are presented in Table 4, and the PDF results from the reliability evaluation of the strength performance in each case are illustrated in Fig. 4.

As shown in Table 4, similar probabilities of reliability were calculated from Cases 1 to 3 when using the SSM and MCS. Furthermore, the PDF results from Cases 1 to 3 based on the SSM and MCS were similar, as shown in Fig. 4. However, the probability of

Table 5 Comparison of Kriging meta-modeling results

Sampling method		# of sampling	R^2 value		
			LC1	LC2	LC3
MCS		158,400	0.995	0.994	0.995
SSM	Case 1	6,144	0.947	0.942	0.941
	Case 2	3,072	0.940	0.939	0.947
	Case 3	1,536	0.930	0.933	0.934
	Case 4	768	0.921	0.913	0.924
	Case 5	384	0.907	0.902	0.911
	Case 6	192	0.852	0.871	0.863
	Case 7	96	0.826	0.835	0.817

reliability of Cases 4 through 7 when using the SSM reduced in proportion to the decrease in the sampling frequency, whereas the probability of reliability tended to be higher than based on the MCS, which can be considered as an indicator of reduced design safety. Additionally, the differences in the PDF results of Cases 4 through 7 obtained using the SSM compared with those obtained using the MCS increased significantly with decreasing sampling frequency. To apply the SSM in the reliability estimation of the AOSC's structural design addressed in this study, it was discovered that at least 1% of the sampling frequency used in the MCS would be required. Therefore, the efficiency of numerical calculations in the SSM-based reliability analysis was high, and the analysis method would be effective for evaluating the structural design safety of fishery equipment, such as AOSCs.

3.3 Comparison of Kriging Metamodeling Characteristics

In this study, a Kriging metamodel was created for each sampling method used for the reliability analysis of the AOSC, and the correlation between the sampling method characteristics and metamodels was reviewed by analyzing the accuracy of the result in each metamodel. Because a Kriging metamodel can approximate multiple design variables and highly nonlinear problems in the design space by incorporating random sampling, Kriging metamodeling was applied to the data used in the random sampling methods, i.e., MCS and SSM (Cho et al., 2009). The accuracy in the design space exploration of the Kriging metal model created for each strength performance response in the design load conditions, i.e., LC1 through LC3, was reviewed based on each of the sampling methods used in the MCS and SSM for reliability analysis. The accuracy of the metamodel approximation was determined in terms of R^2, as shown in the following equation:

$$R^2 = 1 - \frac{\sum(t_i - y_i)^2}{\sum(t_i - \overline{t_i})^2} \tag{13}$$

Here, t_i is an actual value, y_i is a predicted valued in the approximation model, and $\overline{t_i}$ is the mean of the actual values. An R^2 value of 1.0 indicates that the predicted values from the metamodel correspond exactly to the actual values in the entire design space. The accuracy of the Kriging metamodel result for each sampling method is summarized in Table 5. As shown in Table 5, the design space can be approximated with a 0.5% error rate in the MCS with a sampling frequency of 158,400 times, whereas the approximation accuracies from Cases 1 to 3 in the SSM were similar with 5% to 6% higher error rates than those in the MCS. The approximation accuracies of Cases 4 and 5 in the SSM with sampling frequencies of 768 and 384, respectively, tended to exhibit higher error rates of 7 to 9% than in the MCS, respectively. In Cases 6 and 7 with a sampling frequency of 192 or less, the approximation accuracy reduced significantly and was considered to be unsuitable for a metamodel. Although the correlation between the sampling frequency and the accuracy of the Kriging metamodel appeared to be proportional in general, a certain level of sampling frequency would be required to ensure an equivalent level of accuracy in Kriging metamodels, as demonstrated in Cases 1 through 3 in the SSM. Furthermore, as shown in the reliability analysis results in Table 4 and Fig. 4, the SSM incorporating more than 1% of the sampling frequency of the MCS is applicable not only to the reliability analysis, but also to the Kriging metamodeling of the structural design of fishery equipment, such as AOSCs.

4. Conclusions

In this study, reliability analysis was performed by applying a general MCS and the SSM, i.e., a type of quasi-MCS, to derive efficient reliability evaluation methods to ensure the structural design safety of AOSCs. Furthermore, the probability of failure and the accuracy of metamodeling were compared for various sampling frequencies. The key findings of this study are summarized as follows:

(1) The strength performance of the AOSC was evaluated by determining the design load conditions reflecting the actual operating conditions and applying them in a finite element model to calculate the maximum stress under each design load condition. Although the result from the strength performance evaluation satisfied the structural safety standard, a quantitative review of reliability was necessary to address the uncertainties in the design factors because the safety margin of the

strength performance was small.

(2) The thickness of the major structural components of the AOSC was selected as a random variable for reliability analysis, and the strength performance for each design load condition was considered as a probability performance function. Through this reliability analysis, the probability of failure, probability performance function distribution, and efficiency of numerical calculations based on the sampling method were verified by varying the sampling frequency in the SSM and comparing the results to the MCS with a sampling frequency that estimated the reliability with a confidence level of 95% and an error rate of 5%.

(3) To apply the SSM in the structural design of AOSCs, a sampling frequency equivalent to at least 1% of the MCS sampling frequency would be required to achieve the same probability of reliability and PDF results as those of the general MCS method.

(4) Kriging metamodels suitable for the approximation of random sampling data were applied to review the correlation between the characteristics of the design space approximation and the sampling methods as well as to compare the approximation accuracy. Although the correlation between the accuracy of the Kriging metamodels and the sampling frequency was discovered to be proportional in general, the sampling frequency in the SSM should be at least 1% of the MCS sampling frequency to achieve the same level of accuracy as the Kriging metamodels.

(5) Because the SSM is highly efficient for numerical calculations, it is applicable to the reliability analysis of the structural design of fishery equipment, such as AOSCs, as well as to Kriging metamodeling. The results from this study regarding the sampling method requirements for an effective reliability analysis based on the SSM and Kriging metamodeling will be useful for the reliability analysis of other similar fishery equipment using the SSM.

Acknowledgments

This study was conducted with the support of the National Research Foundation of the Korea Onsite Customized Science and Engineering Talent Cultivation Support Program (No.2019H1D8A1105567) and was supported by the Research Funds of MNU Innovative Programs for University in 2020.

References

Bai, Y., Tang, J., Xu, W. & Ruan, W. (2015). Reliability-based Design of Subsea Light Weight Pipeline Against Lateral Stability. Marine Structures, 43(1), 107-124. https://doi.org/0.1016/j.marstruc.2015.06.002

Cho, S,K., Byun, H. & Lee, T.H. (2009). Selection Method of Global Model And Correlation Coefficients for Kriging Metamodel, Transactions of the Korean Society of Mechanical Engineers-A, 33(8), 813-818. https://doi.org/10.3795/KSME-A.2009.33.8.813

DNV-GL. (2015). Structural Design of Offshore Units - WSD Method (DNVGL-OS-C201). Det Norske Veritas AS.

Han, J.W., & Park, Y.S. (2012). Evaluation of Corrosion Characteristics of Pipeline Material (SUS316) for the Geothermal Power Plant. Korean Journal of Air-Conditioning and Refrigeration Engineering, 24(2), 142-146. https://doi.org/10.6110/KJACR.2012.24.2.142

Korea Maritime Institute (KMI). (2019). KMI Trend Analysis. 161, Seoul.

Lee, O.S. & Kim, D.H. (2006). The Reliability Estimation of Pipeline Using FORM, SORM and Monte Carlo Simulation with FAD. Journal of Mechanical Science and Technology, 20(12), 2124-2135. https://doi.org/10.1007/BF02916329

Lee, C.H. & Kim, Y. (2017). Reliability-based Flaw Assessment of a Mooring Chain Using FORM and SORM. Journal of the Society of Naval Architects of Korea, 54(5), 430-438. https://doi.org/10.3744/SNAK.2017.54.5.430

Lee, J., & Song, C.Y. (2013). Estimation of Submerged-arc Welding Design Parameters Using Taguchi Method and Fuzzy Logic. Proceedings of the Institution of Mechanical Engineers, Part B: Journal of Engineering Manufacture, 227(4), 532-542. https://doi.org/10.1177/0954405413476487

Saltelli, A., Annoni, P., Azzini, I., Campolongo, F., Ratto, M. & Tarantola, S. (2010), Variance Based Sensitivity Analysis of Model Output. Design and Estimator for the Total Sensitivity Index. Computer Physics Communications, 181(2), 259–270. https://doi.org/10.1016/j.cpc.2009.09.018

Siddall, J.N. (1983). Probabilistic Engineering Design. Marcel Dekker Inc., New York. https://doi.org/10.1115/1.3269441

Simulia. (2018). Abaqus User Manual. Simulia.

Sobol, I.M. & Levitan, Y.L. (1999). A Pseudorandom Number Generator for Personal Computers. Computers & Mathematics with Applications, 37(4-5), 33–40. https://doi.org/10.1016/S0898-1221(99)00057-7

Song, C.Y., Lee, J., & Choung, J. (2011). Reliability-based Design Optimization of an FPSO Riser Support Using Moving Least Squares Response Surface Meta-models. Ocean Engineering, 38(1), 304-318. https://doi.org/10.1016/j.oceaneng.2010.11.001

Yin, F., Nie, S., Ji, H., & Huang, Y. (2018). Non-probabilistic Reliability Analysis and Design Pptimization for Valve-port Plate Pair of Seawater Hydraulic Pump for Underwater Apparatus. Ocean Engineering, 163(1), 337-347. https://doi.org/10.1016/j.oceaneng. 2018.06.007

Author ORCIDs

Author name	ORCID
Song, Chang Yong	0000-0002-1098-4205